DALTON
FULL PAPER

Rates of solvent exchange in aqueous aluminium(III)–maltolate complexes †

Ping Yu,[a] Brian L. Phillips,[b] Marilyn M. Olmstead[c] and William H. Casey*[a,d]

[a] *Department of Land Air and Water Resources, University of California, Davis, 95616-8627, USA*
[b] *Department of Geosciences, State University of New York, Stony Brook, NY 11794-2100, USA*
[c] *Department of Chemistry, University of California, Davis, 95616-5295, USA*
[d] *Department of Geology, University of California, Davis, USA. E-mail: whcasey@ucdavis.edu*

Received 14th November 2001, Accepted 11th March 2002
First published as an Advance Article on the web 23rd April 2002

Results from single-crystal X-ray diffraction and ^{27}Al- and ^{17}O-NMR spectroscopy are reported for a series of aluminium–maltolate complexes. Maltolate bonds to Al(III) *via* 3-*oxy* and 4-pyronate functional groups and in acidic solutions forms bidentate complexes with Al(III) that have the stoichiometry: $Al(ma)_n(H_2O)_{6-2n}^{3-n}$ (ma = maltolate and n = 0, 1, 2, 3), which was confirmed by the structure refinement of the n = 3 compound. The relative concentrations of these complexes determined by ^{27}Al-NMR compare well with those predicted from thermodynamic data derived from potentiometry at 298 K and I = 0.6. The rate parameters for exchange of inner-sphere water molecules with bulk solution were determined by ^{17}O-NMR for the $Al(ma)(H_2O)_4^{2+}$ complex: k_{ex}^{298} = 304 (±26) s^{-1}, $\Delta H^{\ddagger}$ = 63 (±2) kJ mol^{-1}, and $\Delta S^{\ddagger}$ = 14 (±7) J mol^{-1} K^{-1} and for $Al(ma)_2(H_2O)_2^{+}$: k_{ex}^{298} = 1950 (±91) s^{-1}, $\Delta H^{\ddagger}$ = 49 (±2) kJ mol^{-1}, and $\Delta S^{\ddagger}$ = −19 (±6) J mol^{-1} K^{-1}. Surprisingly, maltolate labilizes inner-sphere water molecules to an extent that is similar to bidentate dicarboxylate and carboxylate plus phenolic ligands studied previously. Substitution of a single maltolate into the inner-coordination sphere of Al(III) increases the exchange rate of the remaining bound water molecules with the bulk solution by a factor of ≈10^2. Substitution of a second maltolate increases the rates by another factor of 6–7, which is similar to simple aliphatic organic acids, such as methylmalonate.

Introduction

Computational methods promise considerable advances in predicting the rates of aqueous reactions, which are particularly important for the geochemistry of natural waters. Potentially useful correlations can be established between calculable molecular properties, such as bond lengths or atomic charges, and measured reaction rate coefficients for model complexes. Since many geochemical processes involve ligand-exchange reactions involving aluminium, we have been determining rates of elementary solvolysis reactions in simple aqueous Al(III) complexes and dissolved multimers. Solvent-exchange reactions are particularly useful because the reactant and product states are identical; variation in the reaction rates with temperature depends only on the energy of a single transition state. This class of reactions provides data to test correlations derived from electronic-structure calculations that might be used to predict rates of reactions in complicated geochemical settings.

In the present study we examine the structure and rates of solvent exchange in aluminium complexes of maltol (3-hydroxy-2-methyl-4-pyrone; CAS #118-71-8):

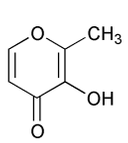

† Electronic supplementary information (ESI) available: equilibrium constants used to model the solution speciation; Al and O speciation in the Al(III)–maltolate complexes based on ^{27}Al-NMR; conditional equilibrium constants for sample 32-66-1 as a function of temperature. See http://www.rsc.org/suppdata/dt/b1/b110457h/

which is a Lewis base that forms strong chelate complexes with Al(III). We chose this ligand because it bonds to Al(III) *via* the 3-*oxy* and 4-pyronate oxygens, which are not represented in any of the other bidentate complexes that have been studied so far. We have previously determined solvent-exchange rates for ligands which bond to Al(III) *via* a pair of carboxylate oxygens,[1,2] or *via* one carboxylate plus one phenolic oxygen.[3] Maltolate is a natural product and was first isolated from larch trees but is now widely used as a food additive.[4] It is also soluble in water, and tris-complexes of maltolate with Al(III) are toxic and cause brain disease[5,6] and kidney damage.[7] Maltolate is particularly interesting to geochemists because it is similar to the central moiety in the flavones that have been used to crystallize kaolinitic clays at room temperature.[8] Although these are very common soil minerals, their synthesis at ambient conditions is a long-standing problem in Earth science.

Experimental

Materials

For ^{27}Al-NMR experiments, stock solutions were prepared by dissolving reagent-grade $AlCl_3 \cdot 6H_2O$, maltol (Aldrich Chemical Company), KCl, HCl, and $MnCl_2 \cdot 4H_2O$ in 18 MΩ water. The compositions were checked by coulometric titration for chloride where possible. The total dissolved aluminium (ΣAl) concentration in the stock solutions was 0.050 M, and solutions were prepared with total dissolved maltol concentrations (ΣL) of 0.100 and 0.125 M. The pH values were determined by Gran titration at 25 and 65 °C, respectively, and were adjusted to the target pH by adding 0.1 M HCl or 0.1 M

Table 1 Solution compositions for NMR experiments. L = maltolate

Sample	ΣAl/M	ΣL/M	ΣMn/M	ΣNa/M	ΣCl^-/M	ΣL/ΣAl	pH
Solutions used for the ^{17}O and ^{27}Al NMR experiments							
32-68-4	0.0526	0.1014	0.2516	0.743	1.322	1.93	2.86
32-66-1	0.0510	0.1001	0.2503	0.553	1.170	1.96	1.88
32-66-5	0.0504	0.1006	0.2519	0.423	1.083	2.00	1.45
32-66-2	0.0504	0.1251	0.2503	0.751	1.306	2.48	2.92
32-68-3	0.0501	0.1254	0.2502	0.501	1.189	2.50	1.16
Solutions used for ^{27}Al NMR experiments only							
32-64-10	0.0500	0.1000	0.2500	0.721	1.289	2.00	2.91
32-64-9	0.0500	0.1000	0.2500	0.653	1.239	2.00	2.38
32-64-5	0.0500	0.1000	0.2500	0.515	1.128	2.00	1.92
32-64-8	0.0500	0.1250	0.2500	0.653	1.207	2.50	2.89
32-64-7	0.0500	0.1250	0.2500	0.498	1.111	2.50	1.82
32-68-1	0.0500	0.1000	0	1.302	1.415	2.00	1.81
32-68–2	0.0500	0.1250	0	1.500	1.553	2.50	2.84

NaOH. The apparent ionic strengths (I) were maintained constant at 1.5 by addition of NaCl (Table 1).

Separate samples were prepared for the ^{17}O-NMR experiments by dissolving solid reagents in 2 cm^3 of distilled water enriched to ~16% in ^{17}O to yield solutions containing ΣAl = 0.05 M and ΣL = 0.100 or 0.125 M. In order to suppress the ^{17}O-NMR signal from bulk water, $MnCl_2{\cdot}4H_2O$ was added as a relaxation agent to samples used for kinetic studies, while ionic strength was maintained constant at I = 1.5. To assess the effect of Mn(II) on the aluminium speciation, samples with, and without, dissolved Mn(II) were prepared and the speciation was determined using ^{27}Al-NMR. However, no significant variation in the aluminium speciation with Mn(II) addition was observed.

X-Ray crystal structures

Crystals of $[Al(maltolate)_3]{\cdot}0.5H_2O$ were grown from a solution containing ΣAl = 0.080 M and ΣL = 0.24 M at pH = 4.4. Crystal data: $C_{18}H_{16}AlO_{9.5}$, M = 411.29, orthorhombic, a = 18.3169(7), b = 11.5723(5), c = 17.6072(7) Å, U = 3732.2(3) $Å^3$, T = 90(2) K, space group $Pca2_1$ (no. 29), Z = 8, μ(Mo-Kα) = 0.162 mm^{-1}, 34581 reflections measured, 11025 unique (R_{int} = 0.052), which were used in all calculations. The final $wR(F^2)$ was 0.082 (all data).

CCDC reference number 181923.

See http://www.rsc.org/suppdata/dt/b1/b110457h/ for crystallographic data in CIF or other electronic format.

Thermodynamic data

Equilibrium constants for the reactions of Al(III) with maltol are reported at 298 K and I = 0.6 in NaCl, and at physiological conditions.[9–13] We use the equilibrium constants of Hedlund and Öhman[9] (Table ESI 1 †), but adjusted them to an apparent ionic strength of 1.5 using the Davies equation:[14]

$$\log \gamma_i = -0.512 Z_i^2 \left[\frac{\sqrt{I}}{1+\sqrt{I}} - 0.3I \right] \quad (1)$$

where γ_i is the individual-ion activity coefficient and Z_i is the charge of the ith solute. For the neutral ligands we used: $\log(\gamma_i) = 0.1{\cdot}I$. Interpretation of the kinetic data is not sensitive to the model chosen for activity coefficient corrections because the concentrations of the $Al(ma)_n(H_2O)_{6-2n}^{3-n}$ species that were used to constrain fits to the ^{17}O-NMR spectra (see below) were determined directly from the ^{27}Al-NMR spectra and not from speciation calculations.

NMR spectroscopy

All NMR experiments were performed on a Bruker Avance spectrometer based on an 11.7 T magnet. The ^{27}Al-NMR spectra were collected using a 10 mm broadband probe (Doty Scientific, Colombia, SC) using single-pulse excitation with a 20 μs pulse (π/2 pulse = 42 μs), a digitization rate of 50 kHz, a relaxation delay of 0.5 s, and 1000 to 2000 acquisitions. The first five points in the time domain were recalculated using a linear-prediction method to remove a baseline roll. An external reference solution of 0.1 M $Al(OH)_4^-$ was used in a coaxial insert to give a peak of constant intensity at δ = 80 ppm in the spectra. Chemical shifts are referenced to this peak position and the integrated relative intensities of all of the ^{27}Al-NMR signals were normalized to the intensity of the external reference. Integrated intensities of peaks in the ^{27}Al-NMR spectra were derived by fitting the observed peaks with Lorentzian functions.

The ^{17}O-NMR experiments were conducted using a GE 10 mm broadband probe with a 20 μs pulse (π/2 pulse ≈ 40 μs), 100 kHz digitization rate, and a 5 ms recycle delay. Typically, 80000 acquisitions were added to yield a reasonable signal-to-noise ratio. Recalculation of the first six points of time-domain data using a linear-prediction algorithm yielded a flat baseline. A coaxial insert of 0.3 M $TbCl_3$ solution, which has a narrow signal at about −100 ppm,[15] was used as an external reference for all the ^{17}O-NMR experiments to give a peak of constant intensity.

Rate coefficients from the ^{17}O-NMR spectra

The average lifetime of a water molecule in the inner-coordination sphere of the complexes was estimated using the dynamic ^{17}O-NMR line-broadening technique.[16–18] In this method ^{17}O-NMR transverse relaxation times (T_2) were obtained directly from the NMR linewidth: $T_2 = (\pi{\cdot}\mathrm{FWHM})^{-1}$, where FWHM is the full-width at half-maximum of the ^{17}O-NMR resonance. The ^{17}O-NMR resonance from bulk water is broadened beyond detection by interaction with Mn(II) species present in the solution.

The relaxation rate includes contributions from both chemical exchange and quadrupolar relaxation:

$$\frac{1}{T_2} = \frac{1}{\tau} + \frac{1}{T_{2,q}} \quad (2)$$

where τ is the mean lifetime of a water molecule in the inner-coordination sphere of the $Al(ma)_n(H_2O)_{6-2n}^{(3-n)+}$ complex, and $\frac{1}{T_{2,q}}$ is the intrinsic quadrupolar-relaxation rate. An Arrhenius-like relation is used to model the temperature dependence of quadrupolar relaxation:

$$\frac{1}{T_{2,q}} = W_{q,298} e^{\frac{E_q}{R}\left[\frac{1}{T} - \frac{1}{298}\right]} \quad (3)$$

where E_q and $W_{q,298}$ are fitting parameters. The temperature dependence of k_{ex} (s^{-1}), the pseudo-first-order rate coefficient

for exchange of water molecules from the inner-coordination sphere to the bulk solution, takes the form of the Eyring equation:

$$k_{ex} = \frac{1}{\tau} = \frac{k_b \cdot T}{h} e^{\frac{\Delta S^{\ddagger}}{R}} e^{\frac{-\Delta H^{\ddagger}}{RT}} \quad (4)$$

where k_b is Boltzmann's constant and the exponential terms include the activation entropy ($\Delta S^{\ddagger}$) and activation enthalpy ($\Delta H^{\ddagger}$) for chemical exchange. The parameters T, R, and h are absolute temperature, the gas constant, and Planck's constant, respectively.

Temperature control

Temperature control was maintained by the standard spectrometer hardware, but the sample temperature was measured independently by placing a copper–constantan thermocouple in the fluid-filled coaxial insert of a sample tube and inserting this apparatus into the sample probe assembly. The accuracy of the temperature is usually ±0.2 K, but we assign an uncertainty ±0.5 K to temperature, and propagate this uncertainty through calculations leading to the rate coefficients, in order to maintain conservative estimates of errors. Uncertainties of 10% in the raw peak widths were also propagated through calculations of rate coefficients. The 10% uncertainty in line widths comfortably spans the range of values that are consistent with reasonable adjustments in spectrum phasing and baseline correction.

Results

Coordination of oxygens to Al(III) in maltolate crystals

The structure of the $Al(ma)_3$ salt (Fig. 1) shows the maltol

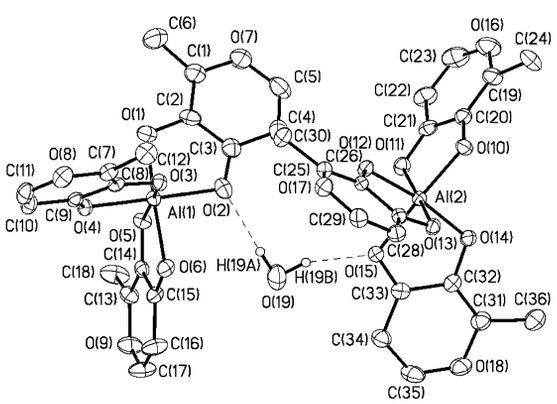

Fig. 1 A drawing of the structure of $Al(ma)_3 \cdot 0.5H_2O$ showing the atom numbering scheme and thermal ellipsoids at the 50% probability level.

ligands in a bidentate arrangement, bonded to the aluminium *via* the 4-pyronate and 3-*oxy* oxygens. The structure presented here differs somewhat from that previously published[19] by the insertion of a molecule of H-bonded water between two distinct Al(ma) complexes (Fig. 1). A somewhat different packing arrangement results, but the metrical parameters for the two structures are similar. In $[Al(ma)_3] \cdot 0.5H_2O$, the water molecule is H-bonded to an acceptor carbonyl oxygen of one ligand in each complex, O(19) ··· O(2) = 2.892(3) Å, O(19) ··· O(15) = 2.814(3) Å. The shorter of the two hydrogen bonds (to O(15)) perturbs the Al–O bond involving this oxygen, as this is the longest Al–O bond (1.968(2) Å) in the structure. Average Al–O distances for the six of each type are 1.939 Å (carbonyl oxygen) and 1.873 Å (deprotonated hydroxy oxygen). The distance between the two Al's in the H-bonded pair is 7.236(2) Å, too long for any cooperative effect. This is not the shortest Al ··· Al distance in the structure, however, as a distance of 6.933(2) Å is obtained from Al(1) ··· Al(2)′ (translated by one unit cell along the *y* direction). Since the maltolate ligand yields a bite angle slightly under 90° (average = 84.8°), the complexes display regular octahedral coordination.

^{27}Al-NMR spectra of variable-pH experiments at 298 K

The ^{27}Al-NMR spectra of Al–maltolate complexes were determined as a function of pH (Fig. 2) to compare with the

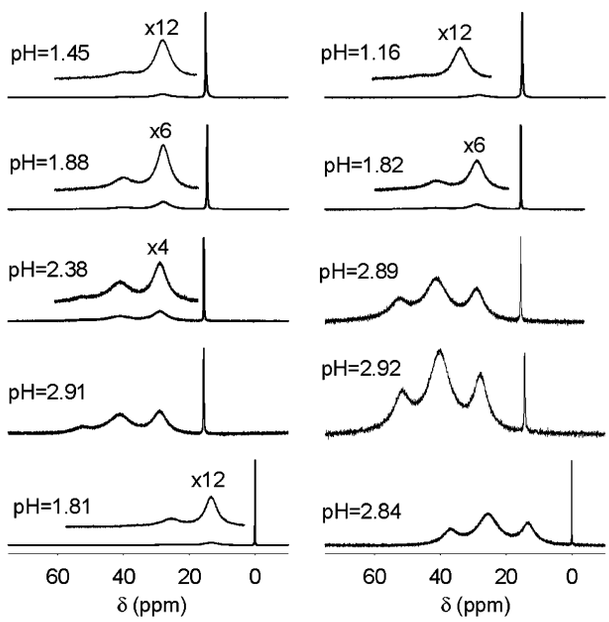

Fig. 2 ^{27}Al NMR spectra as a function of pH at 298 K. Spectra on the left (**a**) correspond to solutions with ΣL/ΣAl = 2.0 and those on the right (**b**) with ΣL/ΣAl = 2.5. From top to bottom, the samples arrayed in (**a**) are: 32-66-5; 32-66-1, 32-64-9, 32-64-10 and 32-68-1 and in (**b**) are: 32-68-3, 32-64-7, 32-64-8, 32-66-2, and 32-68-2. The bottom spectrum in each column is for similar samples that contain no Mn(II).

speciation reported by Hedlund and Öhman[9] and others.[19–21] In the absence of Mn(II), peaks in the ^{27}Al-NMR spectra occur at 0, 13, 26 and 37 ppm (Fig. 2). These peaks are assigned to $Al(H_2O)_6^{3+}$, $Al(ma)(H_2O)_4^{2+}$, $Al(ma)_2(H_2O)_2^{+}$, and $Al(ma)_3$ complexes, respectively.[22] Each peak is well resolved and the relative concentrations of $Al(ma)_n(H_2O)_{6-2n}^{(3-n)+}$ complexes with higher values of *n* increase with pH and with an increased ratio of ΣL/ΣAl, as expected. The speciation of aluminium as a function of pH compares well with calculations using thermodynamic data of Hedlund and Öhman (Fig. 3).[9]

The ^{27}Al-NMR signals for the Al–maltolate complexes are much broader than the peak assigned to the $Al(H_2O)_6^{3+}$(aq) complex (Figs. 2 and 4), which reflects more rapid T_2 relaxation due to larger quadrupolar couplings and slower rates of tumbling of the larger $Al(ma)_n(H_2O)_{6-2n}^{(3-n)+}$ complexes. Some breadth of the ^{27}Al line for the $Al(ma)_2(H_2O)_2^{+}$ complex may also reflect overlapping resonances of the *cis* and *trans* isomers of this species, which we cannot resolve. The paramagnetic Mn(II) causes a constant downfield shift and some additional broadening of all the ^{27}Al-NMR peaks, most likely due to susceptibility effects. However, the relative peak intensities in the ^{27}Al-NMR spectra are virtually unchanged upon addition of Mn(II).

^{27}Al-NMR spectra of variable-temperature experiments

Typical ^{27}Al-NMR peaks for all the Al-maltolate complexes are resolved at temperature from 0 to 80 °C (Fig. 4). The relative intensities of signals for the lower-order complexes, *e.g.*,

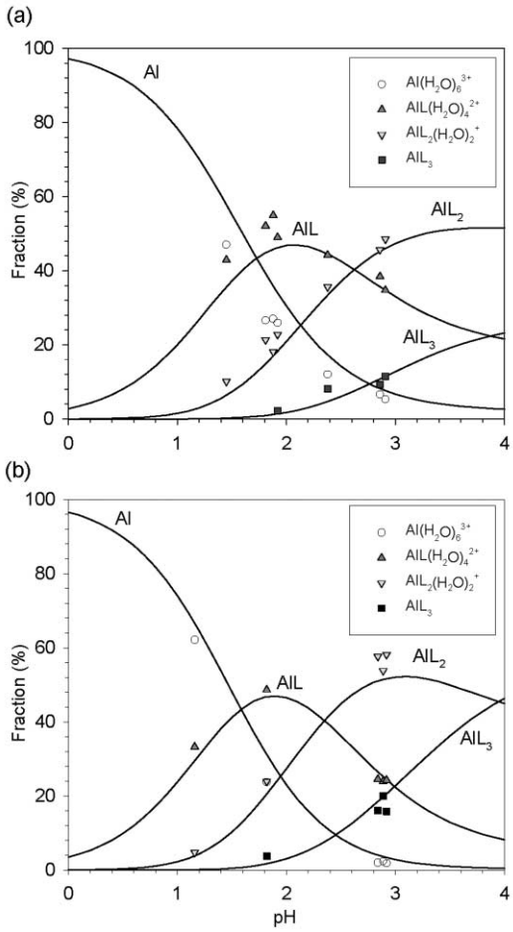

Fig. 3 The aluminium speciation determined from the integrated intensities of peaks in the ^{27}Al-NMR spectra (symbols) compared with thermodynamic calculations at 298 K using the data in Table ESI 1.† The top plot (**a**) is for samples with ΣL/ΣAl = 2 and the bottom plot (**b**) is for samples with ΣL/ΣAl = 2.5.

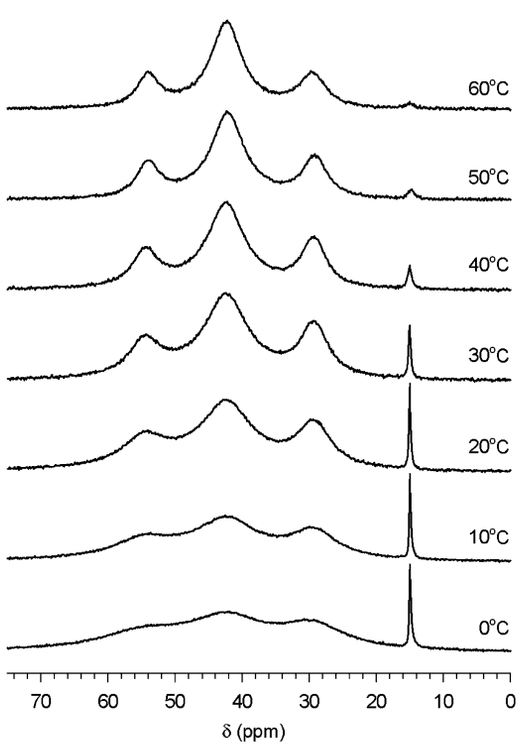

Fig. 4 ^{27}Al-NMR spectra of sample #32-66-2, with ΣL/ΣAl = 2.48 and pH = 2.92 and 0.25 M $MnCl_2$, as a function of temperature.

$Al(H_2O)_6^{3+}$ and $Al(ma)(H_2O)_4^{2+}$, decrease at higher temperatures, indicating that the Al(III) becomes more highly ligated with increased temperature. The difference in chemical shifts among signals for $Al(ma)(H_2O)_4^{2+}$ and $Al(ma)_2(H_2O)_2^{+}$, and $Al(ma)_3$ decreases slightly with increasing temperature. The difference in chemical shifts of $Al(ma)(H_2O)_4^{2+}$ and $Al(H_2O)_6^{3+}$(aq) does not change detectably with temperature. The peak assigned to the $Al(ma)_2(H_2O)_2^{+}$ becomes broader than that for the $Al(ma)_3$ complex above about 10 °C.

Peak widths for all complexes decrease with increasing temperature up to about 40 °C (Fig. 5). However, for samples

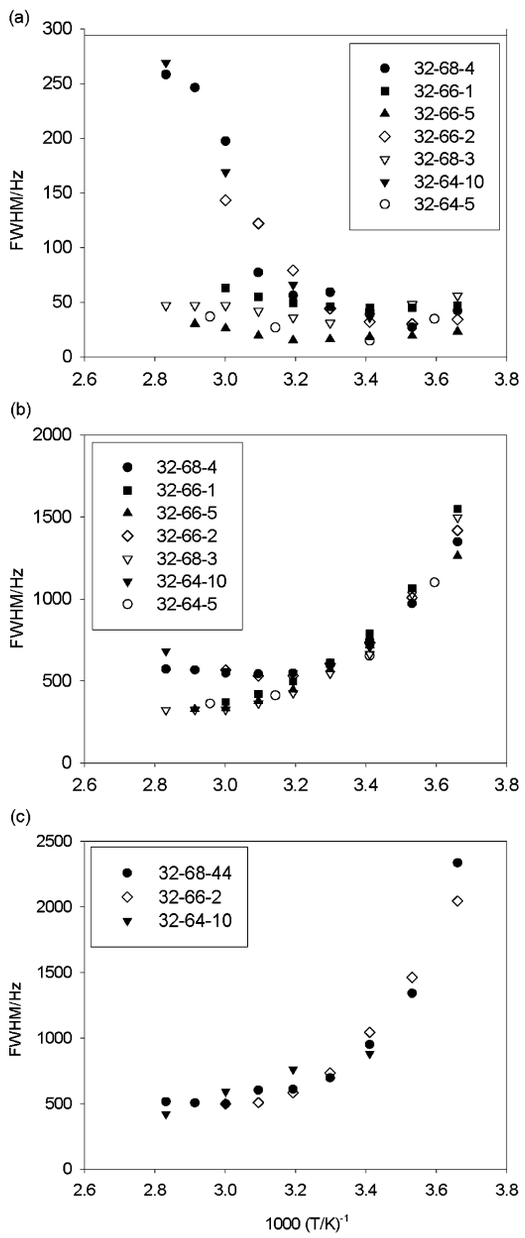

Fig. 5 Widths of peaks in the ^{27}Al NMR spectra that correspond to Al–maltolate complexes as a function of temperature: (**a**) $Al(H_2O)_6^{3+}$(aq), (**b**) $Al(ma)(H_2O)_4^{2+}$, and (**c**) $Al(ma)_3$. The simultaneous broadening of signals for $Al(H_2O)_6^{3+}$(aq) and $Al(ma)(H_2O)_4^{2+}$ complexes at temperatures above 50 °C suggests chemical exchange between aluminium in these two species. The line-broadening for the $Al(H_2O)_6^{3+}$(aq) complex may also contain contributions from hydrolysis. See the text for detail.

with pH > 2.8, the widths for peaks assigned to the $Al(ma)(H_2O)_4^{2+}$ and $Al(H_2O)_6^{3+}$(aq) complexes decrease with increasing temperature up to 40 °C, then increase at higher temperatures (Fig. 5), suggesting the onset of chemical exchange between these two species. Some of the broadening of the peak assigned to the $Al(H_2O)_6^{3+}$(aq) complex can be

attributed to an increase in the concentration of $AlOH(H_2O)_5^{2+}$(aq), which is in rapid exchange equilibrium with the $Al(H_2O)_6^{3+}$(aq) species, since the broadening appears at pH = 3 but not in more acidic solutions.[22,23]

Because we later use ^{17}O-NMR linewidths to determine rates of solvolysis, it is important to evaluate the possible effects of exchange between $Al(ma)(H_2O)_4^{2+}$ and $Al(H_2O)_6^{3+}$(aq) on measurement of the rates of exchange of a solvent water. The rate of exchange (k_{ex}, s^{-1}) of Al(III) from the $Al(H_2O)_6^{3+}$(aq) complex is approximately proportional to the peak broadening due to chemical exchange:

$$k_{ex} = \pi(\Delta FWHM) \quad (5)$$

where ΔFWHM is the difference between the full-width-at-half-maximum for the $Al(H_2O)_6^{3+}$(aq) in the presence, and absence, of exchange.[24] We use the peakwidth at 40 °C as an estimate for the case where there is no chemical exchange and assume that all of the increase in peak widths is due to chemical exchange between $Al(H_2O)_6^{3+}$(aq) and $Al(ma)(H_2O)_4^{2+}$ to obtain a maximum effect. Such a calculation ignores potential contributions to linewidth from an increase in the concentration of $AlOH(H_2O)_5^{2+}$(aq) with temperature, and is thus an overestimate. Nevertheless, broadening of the peak assigned to $Al(H_2O)_6^{3+}$(aq) corresponds to maximum values of ≈200 Hz at 60 °C to ≈700 Hz at 80 °C, which are much slower than the rates of solvent exchange for the $Al(ma)(H_2O)_4^{2+}$ complex over this temperature range.

In very acid solutions (pH ≤ 2.5), the peak width for the $Al(ma)(H_2O)_4^{2+}$ complex decreases over the entire temperature range studied, and that for the $Al(H_2O)_6^{3+}$(aq) increases by only about 15 Hz over the temperature range 40 to 80 °C (Fig. 5). At pH > 2.8 (solutions 32-68-4, 32-64-10 and 32-66-2), the peak width for $Al(H_2O)_6^{3+}$(aq) increases by 190 and 110 Hz, respectively, for the solutions with ΣL/ΣAl ratios of 2.0 and 2.5 (Fig. 5a), which is too large to be only attributable solely to increases in concentration of the $AlOH(H_2O)_5^{2+}$(aq) complex relative to $Al(H_2O)_6^{3+}$(aq).[22,23]

The presence of small concentrations of a monomeric ternary complex might also contribute to the line broadening if deprotonation of a bound water to form a hydroxy caused the rates of ligand exchange to increase. Hedlund and Öhman[9] specifically looked for such a ternary monomer in their potentiometric study and found no evidence. They did, however, find clear evidence of a di-hydroxy-bridged dimer with the stoichiometry: $Al_2(OH)_2(ma)_2^{2+}$(aq) that reaches appreciable concentrations at low pH. We see no evidence of this dimer in either the ^{27}Al- or ^{17}O-NMR spectra, but it may have a resonance that is too broad to observe. Chemical exchange of aluminium sites between this dimer and $Al(H_2O)_6^{3+}$(aq) probably cannot account for broadening of the $Al(H_2O)_6^{3+}$(aq) peak in the ^{27}Al-NMR spectra. The simplest explanation for the observed peak broadening is chemical exchange between the $Al(H_2O)_6^{3+}$(aq) and $Al(ma)(H_2O)_4^{2+}$ complexes. However, for the purpose of the present study, rates of exchange are too slow to significantly influence the ^{17}O-NMR spectra.

Conditional equilibrium constants for the formation of Al–maltolate complexes as a function of temperature can be calculated from the ^{27}Al-NMR peak intensities for the solutions at different pH conditions. Defining conditional equilibrium constants:

$$Al^{3+} + HL \leftrightarrow AlL^{2+} + H^+ \qquad K_1 = \frac{[AlL^{2+}][H^+]}{[Al^{3+}][HL]}$$

$$AlL^{2+} + HL \leftrightarrow AlL_2^{+} + H^+ \qquad K_2 = \frac{[AlL_2^{+}][H^+]}{[AlL^{2+}][HL]}$$

$$AlL_2^{+} + HL \leftrightarrow AlL_3 + H^+ \qquad K_3 = \frac{[AlL_3][H^+]}{[AlL_2^{+}][HL]}$$

and using the measured peak intensities (Table ESI 2†), yields values of K_i that increase with temperature over the range 0–65 °C (Table ESI 3†) corresponding to conditional enthalpies in the range 22 (±2) kJ mol^{-1} for K_1 and 28 (±4) kJ mol^{-1} for K_2.

^{17}O-NMR spectra

The ^{17}O-NMR spectra of Al–maltolate solutions (Fig. 6) exhibit

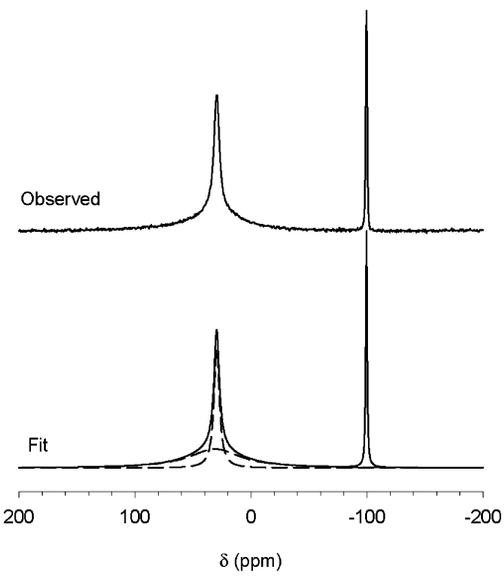

Fig. 6 ^{17}O-NMR spectrum (top) for solution #32-66-1, with ΣL/ΣAl = 1.96 and pH = 1.88, at 70 °C. The bottom figure is a least-squares fit of the spectrum to a sum of three Lorentzian curves. The peak at −100 ppm is due to the external $TbCl_3$ (aq) solution in a coaxial insert. The overlapping resonances in the ^{17}O-NMR spectrum correspond to waters of hydration in the uncomplexed Al(III) ($Al(H_2O)_6^{3+}$ + $AlOH(H_2O)_5^{2+}$ in rapid exchange equilibrium) and $Al(ma)(H_2O)_4^{2+}$ complexes.

a signal near +22 ppm that is a sum of resonances due to waters of hydration in the various aluminium complexes.[1,3,17,18] The second peak, at about −100 ppm, corresponds to a Tb^{3+}(aq) solution that serves as an external standard. We see no ^{17}O-NMR signal from oxygens in the maltolate ligand, even after reacting the uncomplexed ligand (0.05 M) with acidified and ^{17}O-enriched water for a week, which is usually adequate to isotopically equilibrate oxygens in simple carboxylates and amino acids.[25]

Rate coefficients for solvent exchange were estimated from ^{17}O-NMR line widths of the various aqueous complexes. To estimate these linewidths, the ^{17}O-NMR signal from the Al(III) species was fit to a sum of Lorentzian curves using a least-square algorithm (Fig. 6, bottom). The resulting peak widths were used in Equations (2)–(4) to estimate rates of reaction. The presence of the narrow peak from the Tb^{3+}(aq) insert upfield from the bound water peaks enabled the accurate phase adjustments necessary for measuring the width of broad resonances.

Least-squares fits of all ^{17}O-NMR spectra were constrained using data for the estimated concentrations of the $Al(ma)(H_2O)_4^{2+}$, $Al(ma)_2(H_2O)_2^{+}$, and $Al(H_2O)_6^{3+}$ complexes determined from the ^{27}Al-NMR spectra. The contribution of these complexes to the ^{17}O-NMR spectra is determined by their relative abundance in the solution and with the number of bound water molecules in the complex. The measured fractions of various complexes in the ^{27}Al-NMR spectra and their calculated contributions to the ^{17}O-NMR spectra are compiled in Table ESI 2.†

The ^{17}O-NMR transverse-relaxation rates ($1/T_2$) as a function of temperature, determined directly from the peak widths, are plotted in Fig. 7. The $1/T_2$ values display a minimum at

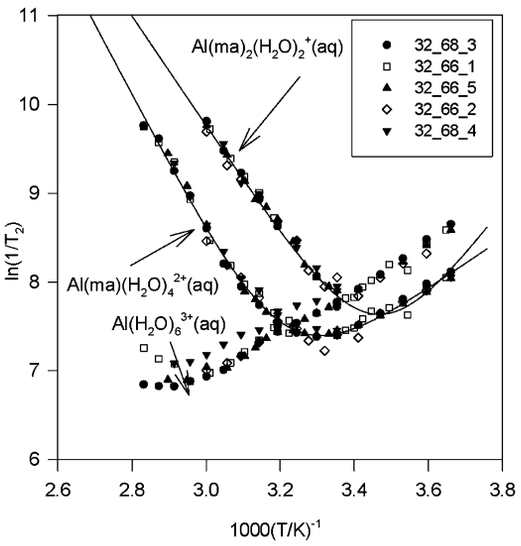

Fig. 7 ^{17}O-NMR transverse relaxation rates ($1/T_2$) for bound waters in the uncomplexed Al(III) (Al^{3+} + $AlOH^{2+}$ complexes), $Al(ma)(H_2O)_4^{2+}$, $Al(ma)_2(H_2O)_2^{+}$ complexes as a function of temperature. Values of $1/T_2$ are obtained from the width of the peaks at 22 ppm returned from the constrained least-squares fits of the spectra to a sum of Lorentzian curves using the constraints on relative concentration of the various complexes derived from ^{27}Al-NMR spectra. The solid lines are fits of the data to Eqns. (2) to (4).

approximately 293 K for the $Al(ma)(H_2O)_4^{2+}$ complex and at approximately 288 K for the $Al(ma)_2(H_2O)_2^{+}$ complex (Fig. 7). At temperatures higher than these minima, the transverse relaxation is dominated by chemical exchange of bound waters with water molecules in the bulk solution. At lower temperatures the $1/T_2$ values are dominated by quadrupolar relaxation. We observed no systematic dependence of relaxation rate on solution pH, indicating that the peaks are not influenced by ternary hydroxy complexes, as was also concluded by Finnegan *et al.*[20] and Hedlund and Öhman.[9] To investigate the possible effect of chemical exchange between $Al(H_2O)_6^{3+}$ and $Al(ma)(H_2O)_4^{2+}$, we simulated spectral components observed at 60 and 80 °C by numerical integration of the Bloch equations, adding chemical exchange between the components at rates of 200 s^{-1} (60 °C) to 700 s^{-1} (80 °C). Least-squares fits of the resulting spectra yielded only a slight increase in the width of the narrower component (due to $Al(H_2O)_6^{3+}$), but no significant change in the width of the broader component ($Al(ma)(H_2O)_4^{2+}$) that was used to obtain rate parameters.

Fits of Eqns. (2) to (4) to these data yield rate parameters for exchange of water molecules from the inner-coordination-sphere of both $Al(ma)(H_2O)_4^{2+}$ and $Al(ma)_2(H_2O)_2^{+}$ with those in the bulk solution. The values for $Al(ma)(H_2O)_4^{2+}$ are: k_{ex}^{298} = 304 (±26) s^{-1}, $\Delta H^{\ddagger}$ = 63 (±2) kJ mol^{-1}, and $\Delta S^{\ddagger}$ = 14 (±7) J mol^{-1} K^{-1}. The parameters for $Al(ma)_2(H_2O)_2^{+}$ complex are: k_{ex}^{298} = 1950 (±91) s^{-1}, $\Delta H^{\ddagger}$ = 49 (±2) kJ mol^{-1}, and $\Delta S^{\ddagger}$ = −19 (±6) J mol^{-1} K^{-1}. The uncertainties were estimated by propagating values of 10% of the raw linewidth and 0.5 K using Monte-Carlo techniques. The rate parameters for the $Al(ma)_2(H_2O)_2^{+}$ complex are the average for two possible isomers (*cis*, *trans*) weighted by their relative concentrations, but we cannot resolve these isomers from one another.

There are several features of these data that indicate that the peak assignments are correct. First, the peak widths for a given complex are also independent of the ΣL/ΣAl ratio of the solutions at a constant temperature, although the relative intensities change. Secondly, the T_2 relaxation rates of the ^{17}O-NMR peak assigned to uncomplexed Al(III) (the peak is a sum of contributions from $Al(H_2O)_6^{3+}$ and $AlOH(H_2O)_5^{2+}$ complexes) in the Al–maltolate solutions are similar to those determined in solutions without maltol.[26]

Discussion

Comparison to other bidentate complexes of Al(III)

Maltolate provides an interesting contrast to the carboxylate or mixed carboxylate plus phenolic complexes that have been examined previously (Table 2) because it bonds to Al(III) *via* a 3-*oxy* atom. The bidentate ligands in Table 2 all bond to Al(III) *via* paired carboxylates (*e.g.*, $Al(ox)^{+}$, $Al(mmal)^{+}$, $Al(mmal)_2^{-}$), or phenol plus carboxylate mixtures ($Al(sal)^{+}$, $Al(ssal)^{+}$), with the exception of maltolate, which bonds *via* 4-pyronate and 3-*oxy* oxygens. These ligands also differ considerably in the size of the chelate ring formed in the bidentate coordination. The chelation rings formed by maltolate and oxalate in bidentate coordination to Al(III) have five atoms, whereas methylmalonate forms a six-membered ring, and both salicylate and sulfosalicylate form seven-membered rings. The extent to which these ligands labilize inner-sphere water molecules does not correlate with the size of the chelate ring.

Although maltolate differs structurally from the other ligands in Table 2, it has a broadly similar effect on the average lifetime of water molecules in the inner-coordination sphere of Al(III) (Table 2). Substitution of a single maltolate ligand into the inner-coordination sphere of Al(III) increases the exchange rate coefficient of the remaining bound water molecules with bulk solution by a factor of $\approx 10^2$. Addition of a second ligand, to form the bis-bidentate complex, $Al(ma)_2(H_2O)_2^{+}$, increases the rates by an additional factor of 6–7.

Surprisingly, the average lifetimes of a water molecule in the $Al(ma)(H_2O)_4^{2+}$ and $Al(mmal)(H_2O)_4^{+}$ (mmal = methylmalonate) complexes are similar to one another even though these complexes differ in net charges and in the size of the chelate ring.

The bis-maltolate and bis-methylmalonate complexes

The $Al(ma)_2(H_2O)_2^{+}$ and $Al(mmal)_2(H_2O)_2^{-}$ species are the only bis-bidentate complexes of Al(III) for which solvent-exchange rate data exist. One anticipates that the Al–O bond lengths to water molecules will be broadly similar in the $Al(ma)_2(H_2O)_2^{+}$ and $Al(mmal)_2(H_2O)_2^{-}$ complexes, since they exhibit similar reactivities.

Karlsson *et al.*[32] reported the structure of a double salt containing $Al(mmal)_2(H_2O)_2^{-}$ anions and $Al(H_2O)_6^{3+}$ cations. In this structure, the two dicarboxylate ligands bonded to Al(III) lie in the equatorial plane and the two water molecules at the apices of the $Al(O)_6$ polyhedra. With this structure one can estimate the extent of Al–O bond lengthening due to coordination to two methylmalonate molecules in the *mer* isomer. Bond lengths to the oxygens in the apical water molecules are 1.935 Å in the $Al(mmal)_2(H_2O)_2^{-}$ anion, and 1.878 Å in the adjacent $Al(H_2O)_6^{3+}$ molecules. The presence of the methylmalonate ligands in *trans* bidentate coordination considerably lengthens the bonds to water molecules in the inner-coordination sphere and increases the rate coefficient for exchange with bulk waters by a factor of ≈7000 (Table 2). These data suggest a strategy for testing *ab initio* calculations to yield rate coefficients. The Al–O bond lengths to water molecules in the $Al(ma)_2(H_2O)_2^{+}$ complex should be similar to those both measured and calculated for the $Al(mmal)_2(H_2O)_2^{-}$ complex and in the range 1.935–1.945 Å. Systematic differences may arise from the effect of solvation, but the differences in bond lengths are easily calculated with existing algorithms.

Conclusions

Maltolate labilizes the inner-sphere water molecules of Al(III) complexes by factors that are very similar to other bidentate ligands, such as methylmalonate, and does not reduce the overall charge of the Al(III) complex as much as previously studied ligands. Substitution of a single maltolate ligand into

Table 2 A compilation of rate coefficients and activation parameters for exchange of water molecules from the inner-coordination sphere of Al(III) complexes to the bulk solution, as determined from ^{17}O-NMR

	Species	k_{ex}^{298}/s^{-1} ($\pm1\sigma$)	$\Delta H^{\ddagger}$/kJ mol^{-1}	$\Delta S^{\ddagger}$/J K^{-1} mol^{-1}	Source
Monomeric complexes with monodentate ligands					
	$Al(H_2O)_6^{3+}$	1.29 (±0.03)	85 (±3)	42 (±9)	17
	$Al(H_2O)_5OH^{2+}$	31000 (±7750)	36 (±5)	−36 (±15)	26
	$AlF(H_2O)_5^{2+}$	240 (±34)	79 (±3)	17 (±10)	27
	$AlF_2(H_2O)_4^{+}$	16500 (±980)	65 (±2)	53 (±6)	27
Monomeric complexes with bidentate ligands					
	$Al(ssal)^{+}$	3000 (±240)	37 (±3)	−54 (±9)	3
	$Al(sal)^{+}$	4900 (±340)	35 (±3)	−57 (±11)	3
	$Al(mmal)^{+}$	660 (±120)	66 (±1)	31 (±2)	2
	$Al(mmal)_2^{-}$	6900 (±140)	55 (±3)	13 (±11)	2
	$Al(ox)^{+}$	109 (±14)	69 (±2)	25 (±7)	1
	$Al(ma)^{2+}$	304 (±26)	63 (±2)	14 (±7)	This paper
	$Al(ma)_2^{+}$	1950 (±91)	49 (±2)	−19 (±6)	This paper
Multimeric complexes					
	Al_{13}	1100 (±100)	53 (±12)	−7 (±25)	28, 29
	$GaAl_{12}$	227 (±43)	63 (±7)	29 (±21)	30
	$GeAl_{12}$	190 (±43)	56 (±7)	20 (±21)	31

Abbreviations: ox = oxalate; ssal = sulfosalicylate; sal = salicylate; mmal = methylmalonate; ma = maltolate; Al_{13} = $AlO_4Al_{12}(OH)_{24}(H_2O)_{12}^{7+}$(aq); $GaAl_{12}$ = $GaO_4Al_{12}(OH)_{24}(H_2O)_{12}^{7+}$(aq) and $GeAl_{12}$ = $GeO_4Al_{12}(OH)_{24}(H_2O)_{12}^{8+}$(aq).

the inner-coordination sphere of Al(III) decreases the average lifetime of water molecules in the inner-coordination sphere by a factor of ≈10^2 and addition of a second maltolate increases the rates by another factor of 6–7.

Acknowledgements

The authors thank Dr. Magnus Karlsson for help in the early stages of these experiments. This work was supported by the U.S. NSF *via* grant EAR 98–14152 and from the U.S. DOE DE-FG03–96ER14629.

References

1 B. L. Phillips, S. Neugebauer-Crawford and W. H. Casey, *Geochim. Cosmochim. Acta*, 1997, **61**, 4965.
2 W. H. Casey, B. L. Phillips, J. P. Nordin and D. J. Sullivan, *Geochim. Cosmochim. Acta*, 1998, **62**, 2789.
3 D. J. Sullivan, J. P. Nordin, B. L. Phillips and W. H. Casey, *Geochim. Cosmochim. Acta*, 1999, **63**, 1471.
4 D. T. LeBlanc and H. A. Akers, *Food Technol.*, 1989, **43**, 78.
5 M. F. Van Ginkel, G. B. Van der Voet, P. C. D'Haese, M. E. De Broe and F. A. De Wolff, *J. Lab. Clin. Med.*, 1993, **121**, 453.
6 B. Corain, G. G. Bombi, A. Tapparo, M. Perazzolo and P. Zatta, *Coord. Chem. Rev.*, 1996, **149**, 11.
7 T. Maitani, T. Suzuki, K. Iwasaki, H. Kubota and T. Yamada, *Jpn. J. Toxicol. Environ. Health*, 1996, **42**, 241.
8 J. D. Hem and C. J. Lind, *Science*, 1972, **184**, 1171.
9 T. Hedlund and L.-O. Öhman, *Acta Chem. Scand.*, 1988, **A42**, 702.
10 G. E. Jackson and C. B. Steyn, *S. Afr. J. Chem.*, 1991, **44**, 110.
11 G. Faraglia, D. Fregona and S. Sitran, *Main Group Met. Chem.*, 1994, **17**, 649.
12 T. G. Lutz, D. J. Clevette, S. J. Rettig and C. Orvig, *Inorg. Chem.*, 1989, **28**, 715.
13 S. L. Phillips, F. V. Hale, F. L. Silvester and M. D. Siegel, *Thermodynamic tables for nuclear waste isolation*, NUREG/CR-4864, U.S. Nuclear Regulatory Commission, Washington DC, 1988, p. 180.
14 C. W. Davies, *Ion Association*, Butterworths, London, 1962, p. 190.
15 C. Cossy, L. Helm and A. E. Merbach, *Inorg. Chem.*, 1988, **27**, 1973.
16 T. J. Swift and R. E. Connick, *J. Chem. Phys.*, 1962, **37**, 307.
17 D. Hugi-Cleary, L. Helm and A. E. Merbach, *Helv. Chim. Acta*, 1985, **68**, 545.
18 B. L. Phillips, W. H. Casey and S. Neugebauer-Crawford, *Geochim. Cosmochim. Acta*, 1997, **61**, 3041.
19 M. M. Finnegan, S. J. Rettig and C. Orvig, *J. Am. Chem. Soc.*, 1986, **108**, 5033.
20 M. M. Finnegan, T. G. Lutz, W. O. Nelson, A. Smith and C. Orvig, *Inorg. Chem.*, 1987, **26**, 2171.
21 E. Chiacchierini and M. Bartusek, *Collect. Czech. Chem. Commun.*, 1969, **34**, 530.
22 J. W. Akitt, *Prog. NMR Spectrosc.*, 1989, **21**, 1.
23 J. W. Akitt and J. M. Elders, *J. Chem. Soc., Faraday Trans.*, 1985, **81**, 1923.
24 J. Sandström, *Dynamic NMR Spectroscopy*, Academic Press, New York, 1982, p. 226.
25 I. P. Gerothanassis, R. Hunston and J. Lauterwein, *Helv. Chem. Acta*, 1982, **65**, 1764.
26 J. P. Nordin, D. J. Sullivan, B. L. Phillips and W. H. Casey, *Inorg. Chem.*, 1998, **37**, 4760.
27 P. Yu, B. L. Phillips and W. H. Casey, *Inorg. Chem.*, 2001, **40**, 4750.
28 B. L. Phillips, W. H. Casey and M. Karlsson, *Nature*, 2000, **404**, 379.
29 W. H. Casey, B. L. Phillips, M. Karlsson, S. Nordin, J. P. Nordin, D. J. Sullivan and S. Neugebauer-Crawford, *Geochim. Cosmochim. Acta*, 2000, **64**, 2951.
30 W. H. Casey and B. L. Phillips, *Geochim. Cosmochim. Acta*, 2001, **65**, 705.
31 A. P. Lee, B. L. Phillips and W. H. Casey, *Geochim. Cosmochim. Acta*, 2002, **66**, 577–587.
32 M. Karlsson, D. Bostrom and L.-O. Öhman, *Acta Chem. Scand.*, 1998, **52**, 995.